Available online at www.sciencedirect.com
ScienceDirect
European Journal of Pharmaceutics and Biopharmaceutics 67 (2007) 9–17
European Journal of Pharmaceutics and Biopharmaceutics
www.elsevier.com/locate/ejpb

Research paper

Preparation and antitumor characteristics of PLA/(PEG-PPG-PEG) nanoparticles loaded with camptothecin

Ryotaro Kunii, Hiraku Onishi *, Yoshiharu Machida

Department of Drug Delivery Research, Hoshi University, Tokyo, Japan

Received 29 May 2006; accepted in revised form 5 January 2007
Available online 28 January 2007

Abstract

Camptothecin (CPT)-loaded nanoparticles were prepared using poly(DL-lactic acid) (PLA) and poly(ethylene glycol)-block-poly(propylene glycol)-block-poly(ethylene glycol) copolymer (PEG-PPG-PEG), and examined for particle characteristics, in vitro release, pharmacokinetics and efficacy. The preparative condition, in which the ratio of PLA/PEG-PPG-PEG/CPT was 35/35/4 (w/w/w) and organic solvent (dichloromethane) was evaporated from the emulsion at 18 °C, gave the nanoparticles with the diameter of approximately 230 nm, fairly high drug content (ca. 1.6% (w/w)) and stable entrapment of the drug, which were used for in vivo studies. After i.v. administration to normal rats, the nanoparticles showed slightly smaller *AUC* but much larger *MRT* as compared with CPT solution, and delivered the drug greatly to the surrounding tissues, in particular to the liver. When antitumor effect was examined by i.v. administration to mice bearing sarcoma 180 (S-180) solid tumor, the nanoparticles showed a significant suppression of tumor growth without body weight loss, and their effect was better than that of CPT solution. The PLA/PEG-PPG-PEG nanoparticles were considered potentially useful to enhance the efficacy of CPT, to which the high drug retention in the body and gradual drug release appeared to be importantly related.

Keywords: PLA/(PEG-PPG-PEG) nanoparticles; Camptothecin; In vitro release; Pharmacokinetics; Antitumor effect

1. Introduction

Camptothecin (CPT), a plant alkaloid isolated from *Camptotheca acuminata*, has been reported to be highly potent in vitro against various tumors by inhibiting the activity of DNA topoisomerase I [1–4]; however, it is not used clinically due to its poor water solubility and to the in vivo low efficacy and severe toxic side effects of its conventional dosage forms [3]. Therefore, its analogues have been produced actively in an attempt to improve CPT characteristics. One of the analogues, irinotecan hydrochloride (CPT-11), exhibits a broad and high antitumor effect in vivo, and is clinically available [5,6]. CPT-11 is regarded as a prodrug of 7-ethyl-10-hydroxycamptothecin (SN-38), being a semi-synthetic derivative of CPT [7–9]. CPT-11 is more than thousand times less effective in vitro than SN-38 and CPT, but is more effective in vivo, which is associated with their pharmacokinetic properties. Namely, SN-38 is eliminated more rapidly from the systemic circulation than CPT-11, while CPT-11 can supply SN-38 at an effective level for a long period [5,6]. Furthermore, SN-38 is more toxic than CPT-11.

As CPT and SN-38 are time-dependently effective [10,11], their prolonged supply is very useful to obtain a higher efficacy. In the previous study [12], CPT-11-loaded nanoparticles were prepared using poly(DL-lactic acid) (PLA) and poly(ethylene glycol)-block-poly(propylene glycol)-block-poly(ethylene glycol) copolymer (PEG-PPG-PEG) in order to improve the efficacy of CPT-11. The CPT-11-loaded nanoparticles showed longer systemic retention of CPT-11 and greater effect against a solid

* Corresponding author. Department of Drug Delivery Research, Hoshi University, 2-4-41 Ebara, Shinagawa-ku, Tokyo 142-8501, Japan. Tel.: +81 3 5498 5724; fax: +81 3 3787 0011.
E-mail address: onishi@hoshi.ac.jp (H. Onishi).

0939-6411/$ - see front matter © 2007 Elsevier B.V. All rights reserved.
doi:10.1016/j.ejpb.2007.01.012

tumor as compared with CPT-11 solution. One reason for the improved efficacy was considered to be enhanced permeability and retention (EPR) effect [13]; that is, nanoparticles with a diameter of some dozen – 400 nm and hydrophilic molecules on the surface tend to exhibit long plasma residence and accumulate more easily into diseased parts such as a solid tumor due to the more permeable blood capillaries and lack of lymphatic drainage, leading to better efficacy against a solid tumor. In addition, we reported that CPT-11-loaded PLA/PEG-PPG-PEG nanoparticles enhanced the in vivo effect of CPT-11 against murine M5076 liver metastasis [14]. This was probably because the nanoparticles enhanced the contact of the drug with the tumor cells. Furthermore, improved efficacy of CPT-11 was also reported in CPT-11-loaded liposomes displaying systemically long retention [15]. However, in those systems loaded with CPT-11, a fairly high dose of CPT-11 or frequent administration was required to obtain a high efficacy, and the improvement was not dramatic [12,14]. This is considered to be because CPT-11 itself is a prodrug of SN-38 and not an active agent. That is, targeting or prolonged supply of active agents such as SN-38 or CPT is considered critical to high enhancement of efficacy. In fact, recently, modification or encapsulation of active agents like CPT, not CPT-11, has been attempted actively; that is, liposomes [16], nanocrystalline suspensions [4], solid lipid nanoparticles [17], polymeric nanoparticles [18] and polymer-drug conjugates [19–21] have been produced to improve antitumor characteristics of CPT or related agents. It was demonstrated that these dosage forms were useful for the enhancement of active agents like CPT. In this study, preparation of PLA/PEG-PPG-PEG nanoparticles loaded with CPT, not CPT-11, was attempted, and the resultant nanoparticles were evaluated based on the in vitro characteristics, pharmacokinetic behaviors and antitumor effects.

2. Materials and methods

2.1. Materials

Poly(DL-lactic acid) (PLA) (MW 10,000) was purchased from Wako Pure Chemical Industries, Ltd. (Osaka, Japan). Poly(ethylene glycol)-block-poly(propylene glycol)-block-poly(ethylene glycol) copolymer with MW 8400 and 80% (w/w) ethylene glycol (PEG-PPG-PEG) was obtained from Aldrich Chemical Company, Inc. (Milwaukee, USA). Camptothecin (CPT) was purchased from Sigma Chemical Co. (St. Louis, USA). All other chemicals were of reagent grade.

2.2. Animals and tumor

Male Wistar rats (6 weeks-old, 200 g) and male ddY mice (6–7 weeks-old, 30–35 g) were purchased from Tokyo Laboratory Animals Science Co. Ltd. (Tokyo, Japan), and bred on the breeding diet MF (Oriental Yeast, Tokyo, Japan) with water ad libitum at 23 ± 1 °C and a relative humidity of $60 \pm 5\%$. They were used for the experiments soon after purchase. The experimental protocol was approved by the Committee on Animal Research of Hoshi University, Japan. The animal experiments were performed in compliance with the Guiding Principles for the Care and Use of Laboratory Animals, Hoshi University, Japan.

Sarcoma 180 (S-180) cells were kindly supplied by Cell Resource Center for Biomedical Research of Tohoku University (Japan) and used as tumor cells. The tumor cells were maintained by intraperitoneal transplantation of 1×10^6 cells suspended in Hanks' balanced solution (0.1 ml) per mouse. In antitumor experiments, S-180 cells (1×10^6 cells) suspended in Hanks' balanced solution (0.1 ml) were inoculated subcutaneously to each mouse at its axillary region.

2.3. Preparation of PLA/(PEG-PPG-PEG) nanoparticles loaded with CPT

Nanoparticles were prepared by O/W emulsification and subsequent evaporation of organic solvent. Two different methods (Methods 1 and 2) were used. Method 1: PLA (35 or 50 mg), PEG-PPG-PEG (21 or 30 mg) and CPT (1, 2 or 4 mg) were dissolved in 8 ml of dichloromethane, and 50 ml of water was added. The mixture was mixed vigorously with a vortex mixer for 30 s, and sonicated at 45 kHz (100 W) for 5 min to obtain the O/W emulsion. These operations were conducted at 25–30 °C. Then, the mixture was stirred at 25–30 °C for 2 h, and condensed with a rotary evaporator under reduced pressure at 35 °C for 1 h. The resultant suspension was separated by gel permeation chromatography (GPC) with a Sephadex G-50 column (2.6 cm in diameter × 15 cm in length) using water as the elution solvent to yield the nanoparticles. Method 2: PLA (35 mg), PEG-PPG-PEG (21 or 35 mg) and CPT (4 mg) were dissolved in 12 ml of dichloromethane. To the resultant solution, 50 ml of water of 37 °C was added, mixed vigorously with a vortex mixer for 30 s, and sonicated at 45 kHz (100 W) for 15 min to obtain the O/W emulsion. The emulsion was stirred at 18 °C for 2 h, and condensed with a rotary evaporator under reduced pressure at 35 °C for 1 h. Finally, GPC was performed for the resultant suspension in the same manner as above to obtain the nanoparticles. Table 1 summarizes preparative conditions for various nanoparticles.

2.4. HPLC assay

High performance liquid chromatography (HPLC) was used for the assay of CPT in the samples. A Shimadzu LC-6 A equipped with a Shimadzu RF-10AXL fluorescence detector (ex. 355 nm, em. 515 nm) and Shimdazu C-R7A plus chromatopac was used. A Waters Nova-Pack C18 (4 μm) column (4.6 mm in diameter × 150 mm in length) was used at 35 °C in a column oven. A mixture of methanol and water (11:9, v/v) with the pH adjusted to 5

Table 1
Particle characteristics of each formulation

Formulation	PLA (mg)	PEG-PPG-PEG (mg)	CPT (mg)	Method	Particle diameter[a] (nm)	Drug content[a] (%, w/w)	Encapsulation[a] efficiency (%)
NP-A	50	30	1	Method 1	230 ± 17	0.14 ± 0.09	11.3 ± 7.3
NP-B	35	21	2	Method 1	217 ± 4	1.32 ± 0.39[*]	38.3 ± 11.3[*]
NP-C	35	21	4	Method 1	217 ± 5	0.19 ± 0.06	2.8 ± 0.9
NP-D	35	21	4	Method 2	234 ± 18	0.84 ± 0.31	12.6 ± 4.7
NP-E	35	35	4	Method 2	228 ± 16	1.59 ± 0.21 [#]	29.4 ± 3.9[#]

[a] The results are expressed as means ± SD ($n = 3$).
[*] $P < 0.05$ vs. NP-A and NP-C.
[#] $P < 0.05$ < vs. NP-D.

using 1 M aqueous acetic acid was used as a mobile phase, and the flow rate was set at 1 ml/min. The absolute calibration curve method was used for the calculation of the concentration.

2.5. Examination of particle characteristics

The size of the nanoparticles was measured by dynamic light scattering of their aqueous suspension with a laser light-scattering instrument, ELS-800, (Otsuka Electronic Co., Ltd., Tokyo, Japan), in which photon correlation was adopted as an analytical method. The drug content was determined as follows: The aqueous suspension of nanoparticles (0.2 ml) was dried under nitrogen gas at room temperature, and the weight of the residue was measured. Then, acetone (2 ml), HPLC mobile phase (1 ml), acetonitrile (3 ml) and 0.15 M aqueous phosphoric acid (2 ml) were added to the residue, and mixed vigorously. To 0.1 ml of the resultant mixture, HPLC mobile phase (4.9 ml) was added and mixed vigorously. The resultant sample (20 μl) was analyzed by HPLC to determine the amount of CPT. The drug content was calculated as the ratio of the CPT amount to the residue weight.

2.6. In vitro release experiments

Two types of nanoparticles (NP-B and NP-E), which showed high drug content, were used for the in vitro release studies. The aqueous suspension of the nanoparticles, obtained by GPC, was diluted with phosphate-buffered saline, pH 7.4, (PBS) to obtain the suspension of 2.8 μg CPT eq./ml. This suspension was divided equally into light-resistant glass tubes. Each tube was set in a water bath warmed to 37 °C, and incubated at 60 strokes per min at 37 °C. At 1 h after the start of incubation, one tube was removed from the water bath, and 0.6 ml of the suspension underwent ultrafiltration gently with an Amicon centrifugal filter device named Microcon YM-100 (MW cut-off 100,000) (Millipore Corp., Billerica, USA) so that some part could be filtered through the ultrafilter. The filtrate (0.1 ml) was mixed with 1 ml of 0.1 M phosphoric acid, and 20 μl of the mixture was analyzed for CPT by HPLC. The same operation was performed at 3, 7 and 24 h after the start of incubation to determine the amount of the released CPT.

2.7. Pharmacokinetic studies in rats

The nanoparticles (NP-E) were used in this experiment. The suspension of nanoparticles was prepared by dilution of the aqueous suspension with saline. CPT solution was prepared using a mixture of saline and dimethylsulfoxide (1:20, v/v) as the solvent. The rats were anesthetized by i.p. injection of pentobarbital at 25 mg/kg (4 ml/kg in saline), and fixed on their back. CPT solution (0.1 ml) or suspension of nanoparticles (0.4 ml) was administered intravenously into the tail vein at a dose of 0.5 mg CPT eq./kg. Blood samples (0.4 ml) were taken with a heparinized syringe at 0.25, 0.5, 1, 3 7, 24 and 48 h after administration for nanoparticles, and at 0.25, 0.5, 1, 2, 4, 7 and 24 h after administration for CPT solution; immediately before each blood sampling, light anesthesia was induced with a small amount of pentobarbital. Plasma was obtained by centrifugation of the blood at 3000 rpm for 15 min. The plasma (0.1 ml) was mixed with 0.1 ml of 0.15 M phosphoric acid, 0.4 ml of acetonitrile was added, and the mixture was stirred vigorously for 1 min. After centrifugation of the mixture at 3000 rpm for 15 min, 0.1 ml of the resultant supernatant was mixed with 70 μl of HPLC mobile phase. The resultant sample (20 μl) was analyzed by HPLC to measure the concentration of CPT for CPT solution and the concentration of total (free plus incorporated) CPT for nanoparticles.

The suspension of nanoparticles was prepared and administered in the same manner as above. At 48 h after administration, the rats were sacrificed by inhalation of ether, and the liver, kidney and spleen were excised and wiped briefly with filter paper. A mixture of saline and 0.15 M phosphoric acid (1:1, v/v) was added to each organ at the same amount, and homogenized using a glass homogenizer with a Teflon pestle. The homogenate (0.1 ml) and 0.15 M phosphoric acid (0.1 ml) were mixed, 0.4 ml of acetonitrile was added, and the mixture was shaken vigorously for 1 min. After the mixture was centrifuged at 3000 rpm for 15 min, the obtained supernatant (0.1 ml) was mixed with 70 μl of HPLC mobile phase. The resultant sample (20 μl) was analyzed for CPT by HPLC.

The recovery of CPT or CPT incorporated in nanoparticles was examined by the addition of known amounts of CPT or nanoparticles to the plasma or homogenate and subsequent assay by HPLC. As to CPT, specified amounts

of CPT were mixed with plasma (0.1 ml) or homogenate (0.1 ml) to give a concentration ranging from 0.5 to 50 ng/ml. In the case of incorporated CPT, specified amounts of nanoparticles were added to plasma (0.1 ml) or homogenate (0.1 ml) to obtain the concentration of 0.5–50 ng CPT eq./ml. The resultant mixture was treated in the same manner as the test samples, and the HPLC assay was performed. The recovery ratio was obtained as a ratio of the observed CPT concentration to the calculated (ideal) one.

The plasma pharmacokinetic analysis was performed for CPT and total CPT after i.v. administration of CPT solution and nanoparticles, respectively. The area under the plasma concentration-time curve $AUC(0–\infty)$, mean plasma residence time $MRT(0–\infty)$, and variance of residence time $VRT(0–\infty)$, expressed by the following equations, were calculated by the trapezoidal rule plus mono-exponential extrapolation to infinity using the pharmacokinetic analysis program MULTI reported by Yamaoka et al. [22].

$$AUC(0–\infty) = \int_0^\infty C_p dt \quad (1)$$

$$MRT(0–\infty) = \int_0^\infty (C_p \times t) dt / AUC(0–\infty) \quad (2)$$

$$VRT(0–\infty) = \int_0^\infty (C_p \times (t - MRT(0–\infty))^2) dt / AUC(0–\infty), \quad (3)$$

where C_p was the plasma concentration of CPT at time t h for CPT solution and that of total CPT at time t h for nanoparticles.

2.8. In vivo antitumor experiments

The nanoparticles (NP-E) were used in this experiment. Saline suspension of nanoparticles (0.4 ml) or CPT solution (0.04 ml) in the mixture of DMSO and saline (20:1, v/v) was administered intravenously to tumor-bearing mice at 2.5 mg CPT eq./kg repeatedly, 7, 9 and 11 d after inoculation (2.5 mg CPT eq./kg × 3). As a control, saline (0.4 ml) was injected intravenously to tumor-bearing mice. The length of the longest tumor axis (L(t), cm) and the length of the axis vertical to the longest tumor axis (W(t), cm) were measured with a caliper square t d after inoculation, and the tumor volume t d after inoculation, (V(t), cm^3), was calculated using the following equation [23].

$$V(t) = L(t) \times (W(t))^2/2 \quad (4)$$

The tumor growth ratio was calculated by $V(t)/V(7)$. Furthermore, the survival time of the mice after inoculation were monitored for 120 d. The mean survival time of the treated group (T) and that of control (C) were examined, and the increase in life span (ILS) was calculated using the following equation:

$$ILS = (T/C–1) \times 100(\%) \quad (5)$$

The ILS values were also used for comparison of antitumor effects.

At the same time, body weight loss was investigated as an index of toxic side effects. Namely, body weight on t d ($B(t)$) was measured t d after inoculation, and the body weight ratio to the initial weight was calculated as $B(t)/B(7)$.

2.9. Statistical analysis

Comparison was performed using the unpaired t-test, and significant difference was set as $P < 0.05$.

3. Results

3.1. Particle characteristics

The nanoparticles were prepared by two methods (Table 1). In Method 1, the evaporation of dichloromethane from the emulsion was performed at 25–30 °C. Each formulation displayed the mean size of 210–230 nm; however, only NP-B displayed good drug content and high encapsulation efficiency. In NP-B, the mean drug content was 1.32% (w/w), and the mean encapsulation efficiency was 38.3% (w/w), while the drug content of NP-A and NP-C was less than 0.2% (w/w). In Method 2, the temperature during the evaporation of dichloromethane from the emulsion was set at 18 °C. From the results in comparison between NP-C and NP-D (Table 1), Method 2 gave a higher content than Method 1. Furthermore, the drug content was raised by the increase in the amount of PEG-PPG-PEG as recognized in Method 2 (NP-D vs. NP-E). NP-E exhibited the highest drug content; though its encapsulation efficiency was somewhat lower than that of NP-B. NP-E possessed unilobed size distribution ranging from 100 to 500 nm with the most frequent distribution between 150 and 250 nm (Fig. 1).

3.2. In vitro release

In this experiment, NP-B and NP-E were used, showing a fairly high drug content. The release tests were performed

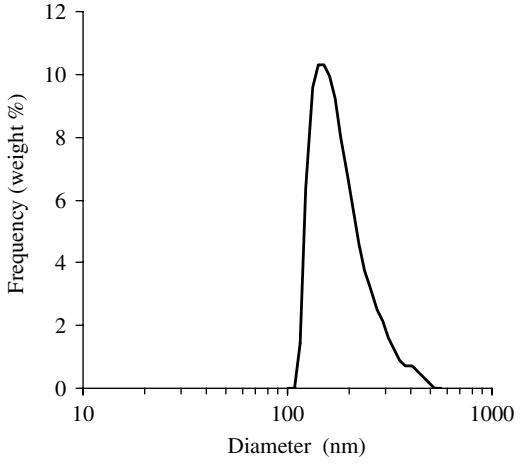

Fig. 1. Partcle size distribution of nanoparticles (NP-E) in weight percent.

using PBS under the conditions in which the concentration of CPT released at 100% was less than the solubility of CPT in PBS at 37 °C. That is, nanoparticles were incubated at the concentration of 2.8 μg CPT eq./ml.

Preliminarily, adsorption properties of CPT to the Microcon YM-100 ultrafilter were examined. After CPT solution with the concentrate of 0.1–3μg/ml in PBS was gently centrifuged using a Microcon YM-100, the fluid remaining without filtration (top part) and the filtrate (bottom part) were analyzed by HPLC. Both parts showed almost the same concentration of CPT. Thus, it was demonstrated that the adsorption of CPT to the Microcon YM-100 ultrafilter was negligible under the present experimental conditions, and the ultrafiltration technique using a Microcon YM-100 was used in the in vitro release studies.

The results in the in vitro release are shown in Fig. 2. NP-B released CPT rapidly; most of the drug was released within 1 h. On the other hand, NP-E exhibited an initial rapid release of approximately 20%, and the remaining CPT was almost maintained in the nanoparticles over 24 h. As to the particle size, the mean size of the nanoparticles NP-E was approximately 230 nm initially, and the size was scarcely changed after the incubation at 37 °C for 24 h.

3.3. Plasma concentration and tissue distribution after i.v. administration in rats

Plasma concentration was monitored after i.v. injection of CPT solution and nanoparticles (NP-E) to rats. The recovery of CPT and incorporated CPT from the plasma was almost 100%. The plasma concentration-time profiles are shown in Fig. 3, in which CPT and total (free + incorporated) CPT are described for CPT solution and nanoparticles, respectively. CPT solution gave plasma concentrations of 185 and 55 ng/ml at 15 and 30 min after

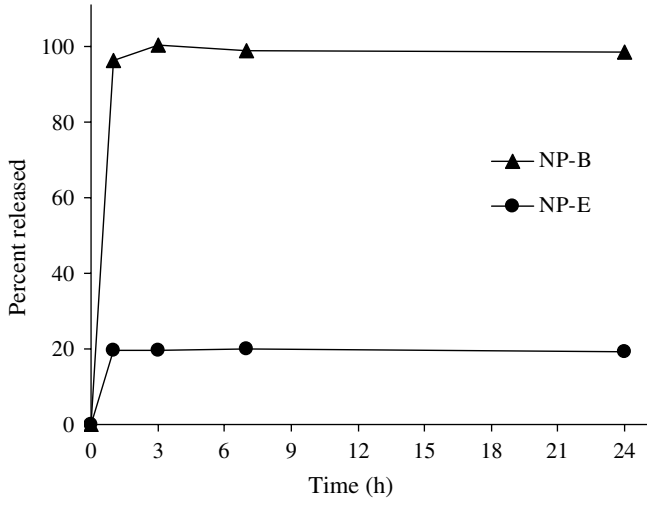

Fig. 2. In vitro release of CPT from nanoparticles (NP-B and NP-E) in PBS at 37 °C. The results are expressed as means ± SD ($n = 3$).

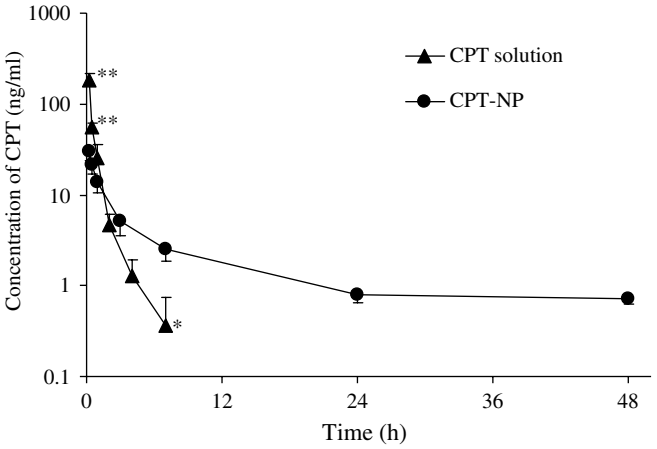

Fig. 3. Plasma concentration of CPT after i.v. injection of CPT solution and nanoparticles (NP-E) at the dose of 0.5 mg CPT eq./kg. Total (free plus incorporated) CPT concentration is shown for nanoparticles. The results are expressed as means ± SE ($n = 4$). $^{*}P < 0.05$ vs. nanoparticles; $^{**}P < 0.01$ vs. nanoparticles.

administration, significantly higher than the total CPT concentration given by nanoparticles ($P < 0.05$). However, at 3 h and later, the total CPT concentration given by nanoparticles was higher than the CPT concentration displayed by CPT solution. The total CPT plasma concentration given by nanoparticles was approximately 2.5 ng/ml at 7 h, and remained at 0.8–0.7 ng/ml from 24 to 48 h.

Pharmacokinetic parameters for the plasma concentration-time profiles of CPT and total CPT were calculated for CPT solution and nanoparticles, respectively (Table 2). The $AUC(0–\infty)$ value of CPT solution was slightly greater than that of nanoparticles; both were not significantly different ($P < 0.05$). The $MRT(0–\infty)$ and $VRT(0–\infty)$ values were much larger in nanoparticles than in CPT solution; each difference was significant ($P < 0.05$).

The tissue concentration of the liver, kidney and spleen was examined at 48 h after i.v. injection (Fig. 4). The recovery ratios of incorporated or total CPT for the nanoparticles were almost 100% in each tissue. The total CPT concentration was more in the order liver > spleen > kidney. The concentration of CPT located in the liver and spleen was much higher than that in plasma.

3.4. In vivo antitumor effect against S-180 solid tumor

Mice bearing S-180 solid tumor with a volume of 0.3–1.0 ml 7 d after inoculation were chosen in this antitumor

Table 2
Moment values for plasma CPT concentration after i.v. administration of CPT solution and nanoparticles (NP-E) at 0.5 mg CPT eq./kg in rats

Formulation	AUC (0–∞) (ng h/ml)	MRT (0–∞) (h)	VRT (0–∞) (h^2)
CPT solution	134 ± 19	0.623 ± 0.157	1.98 ± 1.25
Nanoparticles	127 ± 20	25.1 ± 3.2	1370 ± 270

Total CPT concentration was used for analysis of nanoparticles.

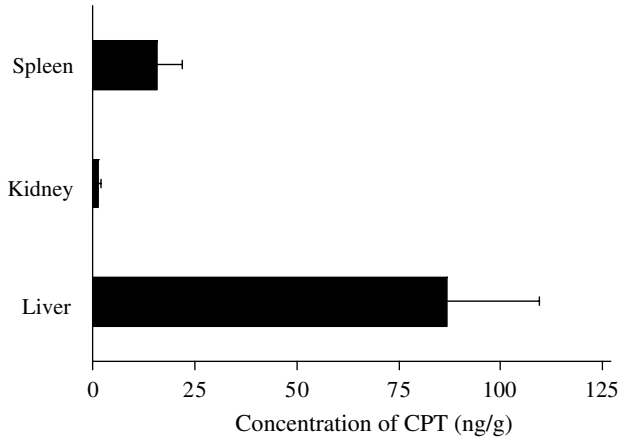

Fig. 4. Tissue concentration of CPT at 48 h after i.v. injection of nanoparticles (NP-E). Total CPT concentration is shown. The results are expressed as means ± SE ($n = 4$).

experiment, and the tumor volume 7 d after inoculation was used as the initial tumor volume. CPT solution and the nanoparticles were administered intravenously to tumor-bearing mice at 2.5 mg CPT eq./kg repeatedly, 7, 9 and 11 d after inoculation, that is, the total dose was 7.5 mg CPT eq./kg. The tumor growth ratios are shown in Fig. 5(a_1 and b_1). In the control, the tumor volume increased approximately 10-fold and 30-fold of the initial volume 20 and 35 d after inoculation, respectively. CPT solution showed good inhibition of tumor growth in the early stage, and suppressed the tumor growth significantly than the control until 22 d after inoculation ($P < 0.05$); however, it subsequently showed no significant difference against the control. The nanoparticles exhibited longer and greater inhibition of tumor growth in comparison with CPT solution, and suppressed tumor volume significantly than the control during the observation period ($P < 0.05$).

At the same time, the body weight was monitored during the above antitumor experiment (Fig. 5(a_2 and b_2)). The body weight 7 d after inoculation was used as the initial body weight. The body weight of the control increased gradually and reached 1.3–1.4-fold of the initial weight 30 d after inoculation. After the third administration of CPT solution 11 d after inoculation, a body weight decreased, but recovered 16 d after inoculation. A significant difference between CPT solution and the control was observed during almost the entire observation time. On the other hand, for the nanoparticles, a decrease in body weight was hardly observed, and the body weight increased gradually at a slower rate than that of the control. There was no significant difference in body weight between nanoparticles and the control except 9 d after inoculation.

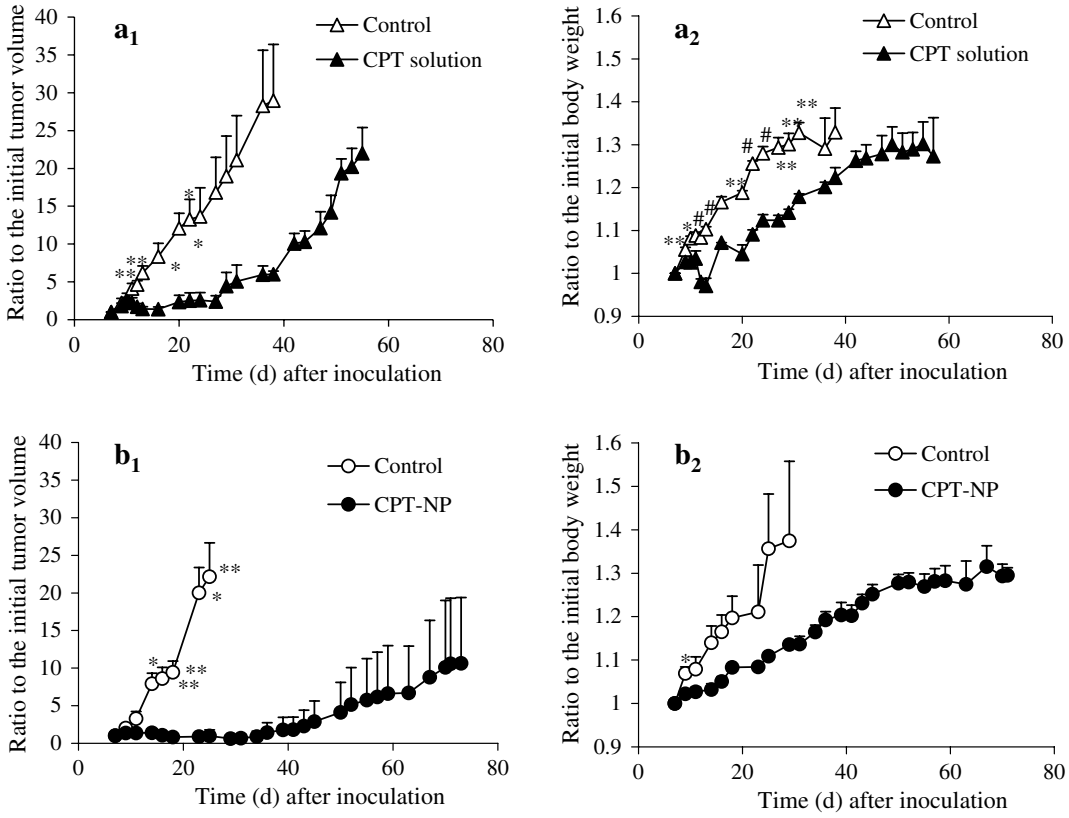

Fig. 5. In vivo antitumor effect of CPT solution (a_1) and nanoparticles (b_1) in mice bearing S-180 subcutaneously and their body weight change with CPT solution (a_2) and nanoparticles (b_2). CPT solution and nanoparticles were administered at a dose of 2.5 mg CPT eq./kg 7, 9 and 11 d after inoculation (total dose = 2.5 mg CPT eq./kg × 3). The results are expressed as means ± SE ($n = 4$ for each control; $n = 3$ for CPT solution or nanoparticles). $^{*}P < 0.05$ vs. control; $^{**}P < 0.01$ vs. control; $^{\#}P < 0.001$ vs. control.

Table 3
Effect of CPT solution and nanoparticles (NP-E) on survival time in mice bearing S-180 subcutaneously

Drug	Survival time (d) of drug after inoculation	Survival time (d) of control after inoculation	ILS (%)
CPT solution	74.7 ± 21.1	44.3 ± 14.2	68.7
Nanoparticles	$102.7 \pm 25.8^{*}$	38.0 ± 15.9	170.2

Survival time was observed for the mice examined in Fig. 5, and is expressed as means ± SD ($n = 4$ for each control; $n = 3$ for CPT solution or nanoparticles).
* $P < 0.01$ vs. control.

In addition, the survival time of the mice used in the above experiment was investigated until 120 h after inoculation. The mean survival time was compared with the control, and the increase in life span was calculated (Table 3). CPT solution and nanoparticles displayed a longer survival time, but only nanoparticles showed significantly prolonged survival time as compared with the control. The *ILS* value of nanoparticles was approximately 2.5-fold greater than that of CPT solution.

4. Discussion

Previously, CPT-11-loaded PLA/PEG-PPG-PEG nanoparticles was developed in order to improve the efficacy and toxicity of CPT-11. The CPT-11-loaded nanoparticles could be prepared readily, probably due to the highly lipophilic properties of the lactone form of CPT-11 [12,14]. The CPT-11-loaded nanoparticles exhibited better efficacy in vivo against both S-180 solid tumor and M5076 liver metastatis in mice [12,14], which was assumed to be due to the long systemic retention of CPT-11 and good accumulation of the drug in the tumor sites. However, a large dose or frequent administration was required to achieve higher efficacy [12,14]. In addition, the CPT-11-loaded nanoparticles did not dramatically improve the efficacy of CPT-11 against S-180 solid tumor. This was considered to be because the cytotoxic action of CPT-11 itself is very low because of its being a prodrug of SN-38 [5,7–9]. Therefore, in this study, preparation of PLA/PEG-PPG-PEG nanoparticles with the active agents related CPT was attempted. First, preparation of SN-38-loaded PLA/PEG-PPG-PEG nanoparticles was attempted, but the nanoparticles having the adequate size and high drug content could not be obtained. This appeared to be associated with the physicochemical properties of SN-38 such as its solubility in the solvent and/or its affinity with the polymer. Next, when using CPT for the preparation of PLA/PEG-PPG-PEG nanoparticles, the nanoparticles with fairly good particle characteristics could be obtained (Table 1). Therefore, in the present study, preparation of PLA/PEG-PPG-PEG nanoparticles containing CPT was studied, and their characteristics were investigated in vitro and in vivo.

The suspension of particles obtained before GPC separation showed the size distribution with more than several μm in addition to that with a few hundred nm. GPC made it possible not only to separate the nanoparticles from free CPT, but also to remove the particles with the size of more than several μm from the nanoparticle fractions which were eluted around the void volume. The particles with the size of more than several μm were considered to be removed by the trapping on the top of or inside the GPC column. Thus, we could obtain the nanoparticles by GPC. The particle size was examined for the nanoparticles obtained by GPC. The particle size, drug content and encapsulation efficiency were dependent on the ratio of CPT and polymers (Table 1). The increase in CPT did not necessarily give a higher drug content as observed in NP-C. There appeared to be an optimal ratio of CPT to polymers. Method 2 seemed to be superior to Method 1 for incorporation of CPT. In the process of emulsification and solvent evaporation, the rate of precipitation of CPT and polymers and the mixing of the precipitated compounds were importantly associated with the quality of the formation of the nanoparticles. Furthermore, the rate of particle formation was considered to be important because large particles were removed. Optimal ratio of PLA/PEG-PPG-PEG/CPT appeared to exist. Particle formation and encapsulation might have been achieved well in NP-B and NP-E. The rate of precipitation of CPT and/or polymers, their mixing and the rate of particle formation were considered to be more suitable in Method 2, probably due to the milder evaporation of the organic solvent.

Drug release was examined in NP-B and NP-E, showing a high drug content (Fig. 2). Ultrafiltration with a Microcon YM-100 was available to separate and determine the released CPT because of no adsorption of CPT to the filter at the experimental condition. NP-B exhibited rapid drug release, and most CPT was released within 1 h. On the other hand, NP-E released approximately 20% of CPT in the initial period, and then the remaining CPT was retained well in the nanoparticles. These suggested that CPT should be better incorporated in NP-E. In NP-B, most of CPT was considered to be located around the surface and/or to be incorporated incompletely. The evaporation process was milder in Method 2 than in Method 1, which might cause a good incorporation of CPT in Method 2. As far as NP-E were observed by transmission electron microscopy, all the particles showed a spherical shape, and no crystal-like particles were observed (data not shown), which also might support the good formation of nanoparticles in NP-E.

Generally, drug release from the PLA core is very slow. In NP-E, after initial rapid release of approximately 20% of the drug, the release of CPT was scarcely observed. Considering the structure of PLA/PEG-PPG-PEG nanoparticles, the core is considered to be mainly composed of PLA molecules. It is suggested that the CPT remaining after initial burst should be incorporated firmly in the PLA core. The in vivo drug release from PLA particles might be different from the in vitro release because of the difference in media. For example, a lipophilic drug can be taken out of the PLA particles in the incubation with cells [24], or surfactants can

act to enhance the drug release [25]. These might have happened to the PLGA microparticles containing glycyrrhetic acid (GLA) reported before [26], because the GLA located in the liver was faster eliminated from the liver than expected from in vitro release rate. Namely, proteins or other surface active materials might make the drug release enhanced in vivo. Therefore, in this study, the nanoparetricles (NP-E) might exhibit a faster drug release rate in vivo as compared with the in vitro one, resulting in the improvement of the drug action.

NP-E had a particle size distribution from 100 to 500 nm with the most frequent distribution between 150 and 250 nm (Fig. 1), which was adequate for passive targeting based on the EPR effect [27,28]. As the particle size was preserved fairly well even after the incubation in PBS at 37 °C for 24 h, suggesting a fairly good physical stability of the nanoparticles.

From these results, NP-E were chosen for the pharmacokinetic experiments and antitumor studies.

After i.v. injection of CPT solution and nanoparticles (NP-E), the plasma level was higher in CPT solution than in nanoparticles for the initial 2 h, but after that, nanoparticles displayed higher plasma concentration (Fig. 3). These plasma concentration-time patterns were fairly similar to those observed in CPT-11-loaded nanoparticles reported previously [12], though the absolute plasma levels were different, partly due to the difference in dose. Namely, the initial plasma concentration was lower but maintained well for a long period in nanoparticles, which was confirmed by the pharmacokinetic analysis as shown in Table 2. The plasma CPT concentration profiles for CPT-loaded methoxypolyethylene glycol-poly(DL-lactic acid) block copolymer (MPEG-PLA) nanoparticles were reported previously after i.v. administration under a similar condition [18]. A slightly higher plasma concentration and retention was observed in MPEG-PLA nanoparticles than in the present nanoparticles. The elimination of PEG-coated nanoparticles from the systemic circulation depends on the density and retention of PEG on the surface of the nanoparticles. PEG-PPG-PEG and PEG-PLA are useful to make the nanoparticles less interactive with cells and retained better in the systemic circulation [18,24,29–31]. However, the protective effect appears greater in PEG-PLA than in PEG-PPG-PEG, because poloxamer 188 is less effective than PEG-PLA to avoid the interaction with cells [24]. This might be one of the reasons that the present nanopraticles exhibited lower plasma levels than MPEG-PLA nanoparticles. When the plasma for nanoparticles was diluted and treated with a Microcon YM-100, CPT was detected for each filtrate (data not shown). The detection of CPT for the filtrate at 7, 24 and 48 h after i.v. administration of the nanoparticles might indicate not only long plasma retention of nanoparticles, but also contribution of the CPT released from the nanoparticles in surrounding tissues.

When the PLA/PEG-PPG-PEG nanoparticles were injected intravenously, the CPT concentration was very high in the liver and spleen in the latter period, for example, the CPT concentration of more than 80 ng/g was observed in the liver even at 48 h after administration at 0.5 mg CPT eq./kg (Fig. 4), which was considered to be due to accumulation of the CPT-loaded nanoparticles into the surrounding tissues. The maintenance of the plasma concentration in the latter phase might be derived from the CPT released from the nanoparticles distributed in the tissues other than blood. As the plasma concentration at a dose of 0.5 mg CPT eq./kg remained constant at 0.8 ng/ml from 24 to 48 h, a higher dose might increase the plasma level to that exceeding the minimum effective concentration, which was 1 – several ng/ml for many tumor cells like KB, P388 and Walker256 cells.

The suppression of tumor growth was better in nanoparticles (NP-E) than in CPT solution as shown in Fig. 5, and this dosing schedule was adequate for treatment using nanoparticles. The lower efficacy of CPT solution was considered to be due to its rapid elimination characteristics (Fig 3). The third administration of CPT solution caused a decrease in body weight, which was considered due to the toxic side effects of CPT. No such decrease in body weight was observed in nanoparticles, which was considered to be because most of the incorporated CPT was released very slowly. Furthermore, ILS was much larger in nanoparticles than in CPT solution (Table 3), which was consistent with the results in the suppression of tumor growth. Thus, the present study suggested that PLA-PEG-PPG-PEG nanoparticles should be useful to improve the efficacy of CPT.

5. Conclusion

The preparation of PLA/PEG-PPG-PEG nanoparticles loaded with CPT was attempted using different methods and conditions, and they were evaluated for particle size, drug content, encapsulation efficiency and in vitro release. When the PLA/PEG-PPG-PEG/CPT ratio was 35/35/4 (w/w/w) and organic solvent in the emulsion was evaporated at 18 °C, nanoparticles showing a good drug content and stable drug retention were obtained. The nanoparticles showed better systemic retention than CPT solution, and delivered CPT into the surrounding tissues to a high extent, in particular into the liver. The plasma CPT levels were fairly low but maintained for a long period, which might be caused by the long systemic circulation of nanoparticles and the recirculation of the drug from the nanoparticles accumulated in surrounding tissues. The antitumor studies with the administration schedules at 2.5 mg CPT eq./kg × 3 d demonstrated that PLA/PEG-PPG-PEG nanoparticles should be useful for the improvement of CPT efficacy.

References

[1] M.E. Wall, M.C. Wani, C.E. Cook, K.H. Palmer, A.T. McPhail, G.A. Sim, Plant antitumor agents: I. The isolation and structure of camptothecin, a novel alkaloidal leukemia and tumor inhibitor from Camptotheca acuminate, J. Am. Chem. Soc. 88 (1996) 3888.

[2] B.C. Giovanella, H.R. Hinz, A.J. Kozielski, J.S. Stehlin Jr., R. Silber, M. Potmesil, Complete growth inhibition of human cancer xenografts in nude mice by treatment with 20-(*S*)-camptothecin, Cancer Res. 51 (1991) 3052–3055.
[3] M. Potmesil, Camptothecins: from bench research to hospital wards, Cancer Res. 54 (1994) 1431–1439.
[4] E. Merisko-Liversidge, P. Sarpotdar, J. Bruno, S. Hajj, L. Wei, N. Peltier, J. Rake, J.M. Shaw, S. Pugh, L. Polin, J. Jones, T. Corbett, E. Cooper, G.G. Liversidge, Formulation and antitumor activity evaluation of nanocrystalline suspensions of poorly soluble anticancer drugs, Pharm Res. 13 (1996) 272–278.
[5] N. Kaneda, H. Nagata, T. Furuta, T. Yokokura, Metabolism and pharmacokinetics of the camptothecin analogue CPT-11 in the mouse, Cancer Res. 50 (1990) 1715–1720.
[6] N. Kaneda, T. Yokokura, Nonlinear pharmacokinetics of CPT-11 in rats, Cancer Res. 50 (1990) 1721–1725.
[7] T. Tsuji, N. Kaneda, K. Kado, T. Yokokura, T. Yoshimoto, D. Tsuru, CPT-11 converting enzyme from rat serum: purification and some properties, J. Pharmacobiodyn. 14 (1991) 341–349.
[8] T. Satoh, M. Hosokawa, R. Atsumi, W. Suzuki, H. Hakusui, E. Nagai, Metabolic activation of CPT-11, 7-ethyl-10-[4-(1-piperidino)-1-piperidino]carbonyloxycamptothecin, a novel antitumor agent, by carboxylesterase, Biol. Pharm. Bull. 17 (1994) 662–664.
[9] L.P. Rivory, M.R. Bowles, J. Robert, S.M. Pond, Metabolic activation of CPT-11, 7-ethyl-10-[4-(1-piperidino)-1-piperidino]carbonyloxycamptothecin, a novel antitumor agent, by carboxylesterase, Biochem. Pharmacol. 52 (1996) 1103–1111.
[10] Y. Kawato, M. Aonuma, Y. Hirota, H. Kuga, K. Sato, Intracellular roles of SN-38, a metabolite of the camptothecin derivative CPT-11, in the antitumor effect of CPT-11, Cancer Res. 51 (1991) 4187–4191.
[11] M. Inaba, Kinetic analysis of cell-killing action of DNA topoisomerase I and II inhibitors, Abstract of Research Works for the General Research A of Subject Number 05302061 with a Grants-in-Aid for Scientific Research from the Ministry of Education, Science, Sports and Culture of Japan. (1994) pp. 57–61.
[12] H. Onishi, Y. Machida, Y. Machida, Antitumor properties of irinotecan-containing nanoparticles prepared using poly(DL-lactic acid) and poly(ethylene glycol)-block-poly(propylene glycol)-block-poly(ethylene glycol), Biol. Pharm. Bull. 26 (2003) 116–119.
[13] Y. Matsumura, H. Maeda H, A new concept for macromolecular therapeutics in cancer chemotherapy: mechanism of tumoritropic accumulation of proteins and the antitumor agent smancs, Cancer Res. 46 (1986) 6387–6392.
[14] Y. Machida, H. Onishi, Y. Kato, Y. Machida, Efficacy of irinotecan-containing nanoparticles prepared using poly(DL-lactic acid) and poly(ethylene glycol)-block-poly(propylene glycol)-block-poly(ethylene glycol) against M5076 tumor in the early liver metastatic stage, S.T.P. Pharma Sci. 13 (2003) 225–230.
[15] Y. Sadzuka, S. Hirotsu, S. Hirota, Effect of liposomalization on the antitumor activity, side-effects and tissue distribution of CPT-11, Cancer Lett. 127 (1998) 99–106.
[16] S.S. Daoud, M.I. Fetouh, B.C. Giovanella, Related articles, antitumor effect of liposome-incorporated camptothecin in human malignant xenografts, Anticancer Drugs 6 (1995) 83–93.
[17] S.C. Yang, L.F. Lu, Y. Cai, J.B. Zhu, B.W. Liang, C.Z. Yang, Body distribution in mice of intravenously injected camptothecin solid lipid nanoparticles and targeting effect on brain, J. Control. Release 59 (1999) 299–307.
[18] H. Miura, H. Onishi, M. Sasatsu, Y. Machida, Antitumor characteristics of methoxypolyethylene glycol-poly(DL-lactic acid) nanoparticles containing camptothecin, J. Control. Release 97 (2004) 101–113.
[19] C.D. Conover, R.B. Greenwald, A. Pendri, C.W. Gilbert, K.L. Shum, Camptothecin delivery systems: enhanced efficacy and tumor accumulation of camptothecin following its conjugation to polyethylene glycol via a glycine linker, Cancer Chemother. Pharmacol. 42 (1998) 407–414.
[20] S. Okuno, M. Harada, T. Yano, S. Yano, S. Kiuchi, N. Tsuda, Y. Sakamura, J. Imai, T. Kawaguchi, K. Tsujihara, Complete regression of xenografted human carcinomas by camptothecin analogue-carboxymethyl dextran conjugate (T-0128), Cancer Res. 60 (2000) 2988–2995.
[21] V.R. Caiolfa, M. Zamai, A. Fiorino, E. Frigerio, C. Pellizzoni, R. d'Argy, A. Ghiglieri, M.G. Castelli, M. Farao, E. Pesenti, M. Gigli, F. Angelucci, A. Suarato, Polymer-bound camptothecin: initial biodistribution and antitumour activity studies, J. Control. Release 65 (2000) 105–119.
[22] K. Yamaoka, Y. Tanigawara, T. Nakagawa, T. Uno, A pharmacokinetic analysis program (multi) for microcomputer, J. Pharmacobiodyn. 4 (1981) 879–885.
[23] Y. Takakura, A. Takagi, M. Hashida, H. Sezaki, Disposition and tumor localization of mitomycin C-dextran conjugates in mice, Pharm Res. 4 (1987) 293–300.
[24] V.C.F. Mosqueira, P. Legrand, R. Gref, B. Heurtault, M. Appel, G. Barratt, Interactions between a macrophage cell line (J774A1) and surface-modified poly (D,L-lactide) nanocapsules bearing poly(ethylene glycol), J. Drug Target. 7 (1999) 65–78.
[25] K. Juni, J. Ogata, M. Nakano, T. Ichihara, K. Mori, M. Akagi, Preparation and evaluation in vitro and in vivo of polylactic acid microspheres containing doxorubicin, Chem. Pharm. Bull. 33 (1985) 313–318.
[26] H. Onishi, H. Takahashi, Y. Machida, Preparation and evaluation of glycyrrhetic acid-containing PLGA microparticles as an anti-hepatotoxic system, Drug Dev. Res. 66 (2006) 189–199.
[27] Y. Tabata, Y. Murakami, Y. Ikada, Tumor accumulation of poly(vinyl alcohol) of different sizes after intravenous injection, J. Control. Release 50 (1998) 123–133.
[28] O. Ishida, K. Maruyama, K. Sasaki, M. Iwatsuru, Size-dependent extravasation and interstitial localization of polyethyleneglycol liposomes in solid tumor-bearing mice, Int. J. Pharm. 190 (1999) 49–56.
[29] S.E. Dunn, A.G.A. Coombes, M.C. Garnett, S.S. Davis, M.C. Davies, L. Illum, In vitro cell interaction and in vivo biodistribution of poly(lactide-co-glycolide) nanospheres surface modified by poloxamer and poloxamine copolymers, J. Control. Release 44 (1997) 65–76.
[30] Z. Panagi, A. Beletsi, G. Evangelatos, E. Livaniou, D.S. Ithakissios, K. Avgoustakis, Effect of dose on the biodistribution and pharmacokinetics of PLGA and PLGA-mPEG nanoparticles, Int. J. Pharm. 221 (2001) 143–152.
[31] C.A. Nguyen, E. Allemann, G. Schwach, E. Doelker, R. Gurny, Cell interaction studies of PLA-MePEG nanoparticles, Int. J. Pharm. 254 (2003) 69–72.